


Estradiol and NADPH oxidase crosstalk regulates responses to high fat feeding in female mice

Martin J Ronis^{1,2,3} , Michael L Blackburn^{1,2}, Kartik Shankar^{1,2}, Matthew Ferguson^{1,2}, Mario A Cleves^{1,2} and Thomas M Badger^{1,2}

¹Department of Pediatrics, University of Arkansas for Medical Sciences, Little Rock, AR 72205, USA; ²Arkansas Children's Nutrition Center, Little Rock, AR 72202, USA; ³Department of Pharmacology & Experimental Therapeutics, Louisiana State University Health Sciences Center, New Orleans, LA 70112, USA

Corresponding author: Martin J Ronis. Email: mronis@lsuhsc.edu

Impact statement

Estrogens are known to regulate body composition. In addition, reactive oxygen species (ROS) produced by the action of NADPH oxidase (NOX) enzymes have been linked to obesity development. We examined development of obesity and adipose tissue injury in response to feeding "Western" diets high in fat and cholesterol in intact, ovariectomized (OVX), and estrogen-replaced (OVX + E2) wild type and $p47^{phox-/-}$ female mice where NOX2 activity is inhibited. Weight gain, gonadal fat pad weight, and adipose tissue inflammation were greater in intact WT vs. $p47^{phox-/-}$ mice. Genotype effects on body weight/fat mass were abolished after OVX and restored in OVX + E2 mice. These data indicate adipose tissue responses to feeding the "Western" diet is regulated by negative cross-talk between NOX-dependent ROS signaling and E2-signaling during development. Loss of estrogens post menopause may increase the risk of obesity and metabolic syndrome as the result disinhibition of ROS signaling.

Abstract

We previously demonstrated protection against high fat-induced obesity in female but not male $p47^{phox-/-}$ mice lacking NADPH oxidase NOX1/2 activity. To test the role of estradiol (E2)-NOX crosstalk in development of this sexually dimorphic phenotype, we fed diets containing 42% fat/0.5% cholesterol to intact and ovariectomized wild type female C57BL/6 mice and female $p47^{phox-/-}$ mice and to ovariectomized mice where the diet was supplemented with an 1 mg/kg 17 β estradiol (E2) for 12 weeks from PND28. Weight gain, gonadal fat pad weight, serum leptin and adiponectin, and adipose tissue inflammation were greater in intact wild type vs. $p47$ mice ($P < 0.05$). Genotype effects on body weight/fat mass were abolished after ovariectomized and restored in OVX + E2 mice ($P < 0.05$). The mRNA of downstream PPAR γ targets CD36, lipoprotein lipase, and leptin was higher in intact wild type vs. $p47^{phox-/-}$ mice ($P < 0.05$). Likewise, intact high fat-fed wild type mice had higher expression of the cytokine *Mcp1*; the pyroptosis marker *Nlrp3* and matrix remodeling and fibrosis markers *Mmp2*, *Col1A1*, and *Col6a3* mRNAs ($P < 0.05$). These genotype effects were reversed and restored by ovariectomized and OVX + E2, respectively ($P < 0.05$). These data suggest that triglyceride accumulation in adipose tissue and development of adipose tissue injury in response to feeding diets high in fat and cholesterol is regulated by the balance between NOX-dependent reactive oxygen species signaling and E2-signaling during development. Loss of estrogens post menopause may increase the risk of obesity and metabolic syndrome as the result disinhibition of reactive oxygen species signaling.

Keywords: Estradiol, NADPH-oxidase, adiposity obesity

Experimental Biology and Medicine 2019; 244: 834–845. DOI: 10.1177/1535370219853563

Introduction

Estrogens are known to regulate body composition and energy utilization during development.¹ Loss of estrogens as the result of aromatase deficiency results in the development of metabolic syndrome in both mice and humans accompanied by increased adiposity and development of insulin resistance. These effects are reversed by estrogen treatment.¹ In addition, estrogens have been shown to

have anti-adipogenic and anti-inflammatory properties in adipose tissue.^{2–6} Weight gain, adiposity, and risk of metabolic syndrome also increased in women post-menopause.^{7–9} This has been suggested to be associated with estrogen loss. Obesity-associated metabolic syndrome has also been linked to development of oxidative stress produced as the result of production of reactive oxygen species (ROS) by NADPH oxidase (NOX) enzymes NOX2 and

NOX4.^{10–13} NOX enzymes are a major source of ROS in many cell types.¹⁴ The best characterized NOX enzyme is NOX2 in macrophages which forms superoxide as part of the bactericidal “respiratory burst.”¹⁵ However, NOX2 and additional homologues also have been identified in non-phagocytic cells including preadipocytes, mature adipocytes, and endothelial cells in adipose tissues.^{14,16} Most NOX enzymes including NOX2 are multiprotein complexes in which cytosolic regulatory components assemble with a membrane anchored flavocytochrome b558 (*gp91^{phox}* + *p22^{phox}*) to form superoxide from molecular oxygen which may then be converted to hydrogen peroxide (H_2O_2) through the action of superoxide dismutase.^{14,16} Cytosolic adaptor proteins *p47^{phox}* and *p67^{phox}* translocate from the cytosol to the membrane during NOX2 activation and are required for superoxide production.¹⁶ In addition, a member of the Rho family of small GTPases, Rac1 is required for NOX2 activation.¹⁴ In contrast to NOX2, NOX4 which is also expressed in preadipocytes and mature adipocytes, does not require cytosolic adaptors, produces H_2O_2 rather than superoxide and NOX4-dependent ROS formation parallels NOX4 mRNA expression.^{14,17} It has been suggested that the two enzymes may act in sequence or in parallel to activate different MAP kinase signaling pathways.¹⁵

NOX4 expression was reported as elevated in mouse models of obesity and in obese Pima Indians.¹¹ Moreover, *in vitro* studies suggest that NOX4 is necessary for adipocyte differentiation and that induction of NOX4 activity in mature adipocytes results in release of chemotactic factors such as monocyte chemoattractant protein-1 (MCP-1).¹⁸ The importance of adipocyte NOX4 in development of metabolic syndrome in obesity was recently confirmed in high fat feeding studies in male mice where NOX4 was ablated specifically in mature adipocytes.¹⁹ Although adipocyte differentiation in these mice was unaffected, these mice showed a delayed development of insulin resistance and adipose tissue inflammation during the development of obesity.¹⁹ In contrast, whole body NOX4 knockout mice were observed to have increased whole body energy efficiency and a predisposition towards obesity indicating the importance of NOX4 in other cell types such as hepatocytes in regulation of energy balance.^{20,21}

In contrast, phenotypic data from whole body NOX2-inactivated and NOX2 knockout mice in response to high fat feeding have been variable, perhaps as the result of differences in diet composition (e.g. differences in %fat, fat + cholesterol), developmental window of feeding (beginning at weaning vs. adulthood) and sex, but generally suggest reduced adiposity, reduced adipose tissue inflammation, and increased insulin sensitivity.^{22–24} At least some of the protective effects of NOX2 ablation on adipose tissue inflammation and glucose homeostasis appear to be associated with NOX2 activity in myeloid cells as opposed to adipocytes. Recent high fat feeding studies in male mice where NOX2 was specifically deleted in myeloid cells report delayed development of adiposity and macrophage infiltration of fat pads, decreased inflammation and necrosis in visceral adipose tissue and attenuation of high fat effects on glucose homeostasis.²⁵

Much less information is available on the role of NOX-derived ROS signaling in the effects of high fat feeding in females as compared to males. Previous studies from our laboratory demonstrated the development of a sexually dimorphic phenotype in *Ncf1* (C57BL/6J-*Ncf1^{MJ}*/J) *p47^{phox}* knockout mice (*p47KO*), which have inactive NOX2 as a result of ablation of the *p47^{phox}* protein, when these mice were fed a “Western” diet high in fat and cholesterol during development.²⁶ Female *p47KO* mice were protected against the development of obesity and metabolic syndrome, whereas male obesogenic responses to the high fat diet were considerably less affected by this genotype.²⁶ Dramatic differences in genes regulating adipogenesis and regulating lipid and carbohydrate metabolism were observed in white adipose tissue from female wild type and *p47KO* mice without differences in food intake suggesting cross-talk between estrogens and NOX2-mediated ROS-signaling pathways in regulation of adipose tissue responses to high fat feeding.²⁶ The current study was designed to test this hypothesis directly by examining responses to feeding of the “Western” diet in female wild type and *p47KO* mice after ovariectomy (OVX) with or without 17 β -estradiol (E2) replacement.

Materials and methods

Mice and diets

These experiments were approved by the Institutional Animal Care and Use Committee at the University of Arkansas for Medical Sciences and conducted in an Association of Laboratory Animal Care-approved animal facility under a constant temperature of 22°C and a 12-h light/dark cycle. Time-impregnated C57BL/6 (WT) and C57BL/6J-*Ncf1^{MJ}*/J (*p47KO*) mice were obtained from Jackson labs (Bar Harbor, ME), housed in polycarbonate cages and fed standard rodent chow throughout pregnancy and lactation. After weaning on postnatal day 28, female pups of each genotype were randomized into three groups of *n* = 6–8. One group remained intact, while the remaining two groups underwent OVX. One of the OVX groups of each genotype was fed diets supplemented with E2 at a level of 1 mg/kg diet. All three groups of mice were then fed a “Western” high fat diet (Harlan Teklad TD88137) *ad libitum* for the next 12 weeks. The high fat diets contained 42% fat calories mainly from milk fat and 0.5% cholesterol with casein as the sole protein source. Body weight was recorded on a weekly basis. Food intake was increased by OVX and suppressed by E2 treatment but was found to be unchanged between genotypes with the same estrogenic status. After 10 weeks on diet, mice were placed into metabolic chambers using the Complete Lab Animal Monitoring System (CLAMS) to assess oxygen consumption (VO₂); respiratory exchange ratio (RER); energy expenditure (Heat) and activity. After 11 weeks on diet, all three groups of each genotype: High Fat (HFD), High Fat/OVX (HFD/OVX), and High Fat/OVX/E2 (HFD/OVX/E2) were fasted overnight and submandibular blood drawn for determination of resting blood glucose and insulin. This was followed by oral glucose tolerance testing.²⁷

An i.p. bolus of 1.5 g/kg glucose was administered. Submandibular blood was drawn at 0, 10, 15, 20, 30, 60, and 120 min following glucose challenge for measurement of glucose and insulin. After 12 weeks on diet, the mice were killed, abdominal, gonadal, and subcutaneous fat pads were collected, weighed and stored at -70°C until use. In addition, a piece of the gonadal fat pad was fixed in buffered alcoholic formalin for four days and embedded in paraffin; 6 μm sections were stained with hematoxylin and eosin for morphological examination. Diameters of adipocytes were measured under a Zeiss Axiovert microscope (Carl Zeiss, Thornwood, NY). A minimum of 300 cells at random were measured for each slide and the percentage of cells in each size range compared with MS Excel (Microsoft, Richmond, WA). Crown-like structures representing an accumulation of macrophages around dead adipocytes were identified and scored as described by Giordano *et al.*²⁸ in five 10x fields/sample.

Biochemical analysis

Serum glucose concentrations were analyzed using glucose reagent IR071-072 (Synermed, Westfield, IL). Serum insulin and leptin concentrations were measured using ELISA kits from Linco Research (St. Charles, MO). Serum adiponectin was measured using an ELISA kit from B-bridge International (Sunnyvale, CA).

Real-time RT-PCR

Total RNA was extracted from gonadal fat pads using TRI reagent and cleaned using RNeasy columns (Quiagen, Valencia, CA). RNA quality was ascertained spectrophotometrically (ratio of A260/A280) and also by checking ratio of 28S to 18S ribosomal RNA using the RNA NanoChip on a 2100 Bioanalyzer (Agilent Technologies, Palo Alto, CA). Reverse transcription to cDNA was performed using the iScript Reverse Transcription kit (Bio-Rad Laboratories, Hercules, CA). cDNA was utilized for real-time PCR (RT-PCR) with 2X SYBR green master mix on an ABI Prism 7000 sequence detection system (Applied Biosystems, Foster City, CA). Gene specific oligonucleotide probes were designed using Primer Express Software (Applied Biosystems) (Supplementary Table 1). Relative amounts of mRNA target expression were quantitated using a standard curve according to manufacturer's instructions and normalized against expression of 18S rRNA.

Statistical analysis

Data are presented as mean \pm SEM. Analysis of variance (ANOVA) was utilized to test overall mean differences based on genotype (WT vs. p47KO), estrogen status (Intact vs. OVX vs. OVX +E2), and genotype \times estrogen status interactions. Additional comparisons of differences in means associated with OVX or E2 treatment within genotypes were performed by two-way ANOVA followed by an all pair-wise Student-Newman-Keuls comparison test and considered significant if $P \leq 0.05$. *t* tests were used to compare differences between genotype within the same

treatment group and considered significant if $P \leq 0.05$. Statistical analysis was performed using SigmaStat 3.3 software (Systat Software, San Jose, CA).

Results

Interaction of NOX2 and E2 signaling regulates body weight gain and fat storage in adipose tissues in female mice fed high fat "Western" diets

p47KO mice are a well characterized mouse model in which NOX2-dependent ROS production is abolished in all tissues as the result of loss of the p47^{phox} cytosolic co-factor which is essential for assembly of the NOX2 membrane complex and ROS production.²² In agreement with our previous study, body weight of intact female HFD mice during 12 weeks of feeding was significantly greater than that of female HFD p47KO mice at all ages (body weight 27 ± 2 vs. 20 ± 1 g, HFD vs. HFD p47KO groups at sacrifice, $P < 0.05$) (Figure 1(a)). In contrast, after OVX, although WT weights were slightly lower than p47KO mice up to eight weeks of age, thereafter body weight of HFD/OVX and HFD/OVX p47KO groups did not differ and increased to 32 ± 1 g in both groups at sacrifice. The p47KO genotype effect disappeared (Figure 1(b)). E2 replacement in the diet suppressed body weight in both genotypes and restored the significant difference in body weight between genotypes after 17 weeks of age (body weight 24 ± 1 vs. 20 ± 1 g, HFD/OVX/E2 vs. HFD/OVX/E2 p47KO groups at sacrifice, $P < 0.05$). Genotype differences dependent on the presence or absence of E2 were also observed in the relative weight of the abdominal and gonadal fat pads (Table 1). ANOVA analysis for abdominal fat pads genotype effect $P = 0.08$; effect of estrogenic status $P = 0.003$; interaction $P = 0.2$. OVX significantly increased % abdominal fat pad weight in both WT and p47KO mice and there was no genotype difference in HFD/OVX vs. HFD/OVX p47KO groups. In contrast, E2 replacement reduced % abdominal fat pad weight in p47KO, but not WT, mice and abdominal fat pad weight was greater in the HFD/OVX/E2 vs. HFD/OVX/E2 p47KO group ($P < 0.05$) (Table 1). In the gonadal fat pad, ANOVA analysis for genotype effect $P = 0.17$; effect of estrogenic status $P = 0.001$; interaction $P = 0.04$. OVX increased relative weight only in the HFD/OVX p47KO group vs. HFD/OVX group ($P < 0.05$). E2 replacement reduced relative gonadal fat pad weights in both WT and p47KO OVX/E2 groups relative to the HFD/OVX groups of each genotype ($P < 0.05$), but gonadal fat pad weight was lower in the HFD/OVX/E2 p47KO group relative to the HFD/OVX/E2 group ($P < 0.05$) (Table 1). When data from abdominal and gonadal fat were combined (fat in the visceral compartment (Figure 2)), ANOVA analysis for a genotype effect was $P = 0.09$, for an effect of estrogenic status $P = 0.003$ and for interaction $P = 0.06$. Comparison of genotype effect within HFD/OVX/E2 groups ($P < 0.05$). In contrast to abdominal and gonadal fat pads, relative weight of the subcutaneous fat pads in female HFD mice did not differ statistically by OVX, E2 replacement, or by P47^{phox} genotype (Table 1). In addition to significant interactions between E2

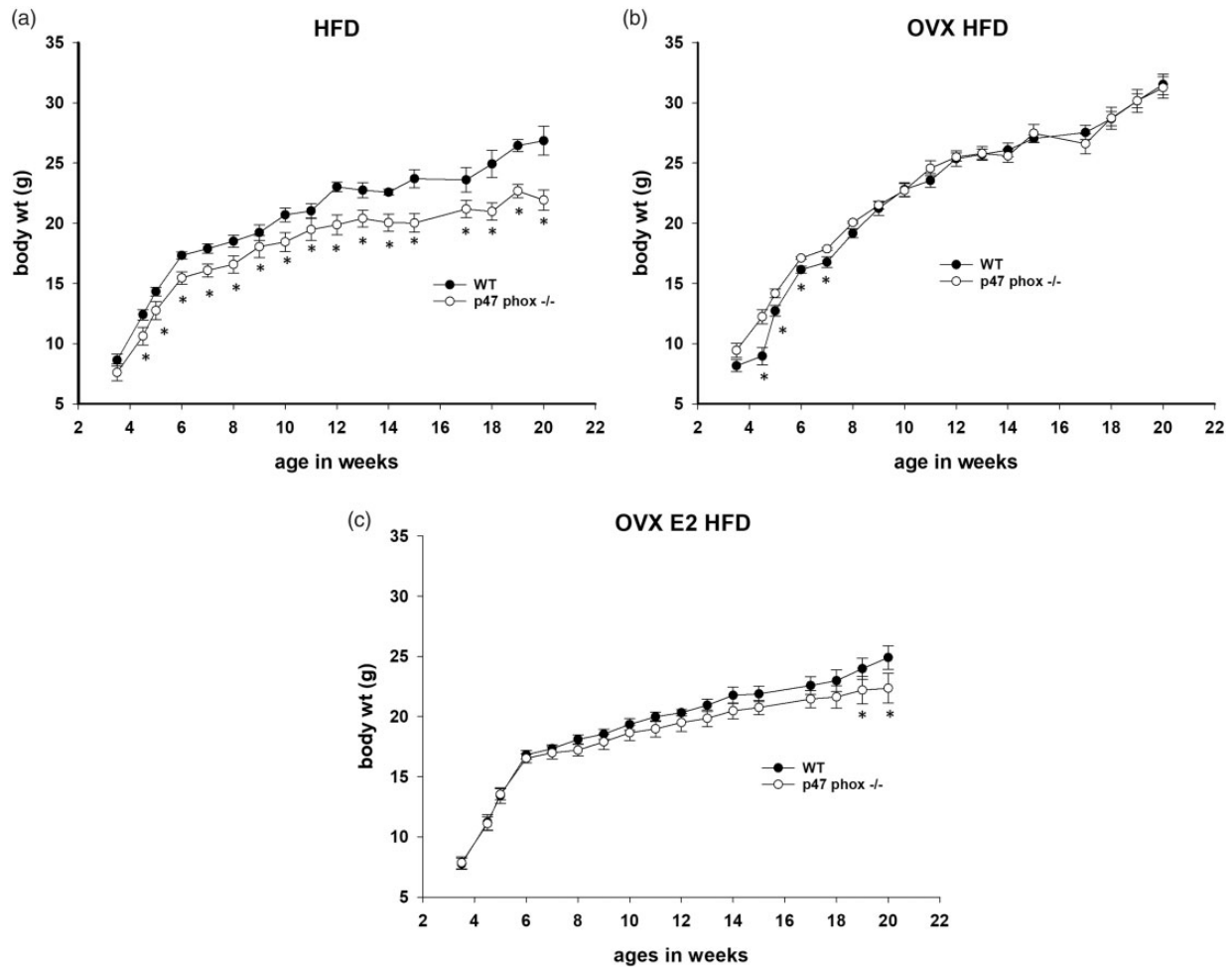


Figure 1. Effects of p47^{phox} genotype and estrogen status on body weight gain in female mice fed high fat “Western” diets. WT: wild type; p47 KO: p47^{phox} ^{-/-} mouse; HFD: high fat diet; OVX: ovariectomy; OVX E2: ovariectomy with estrogen replacement. (a) Intact mice, $P < 0.05$ WT vs. p47^{phox} ^{-/-} mice. (b) OVX mice, NS WT vs. p47^{phox} ^{-/-} mice. (c) OVX E2 mice, $P < 0.05$ WT vs. p47^{phox} ^{-/-} mice. Data are mean \pm SEM for $n = 9$ /group. * Genotype difference in body weight $P < 0.05$.

Table 1. The relationship between estrogen status, p47^{phox} genotype, and fat pad size after feeding HFD.

Fat pad	Genotype	Intact	OVX	OVX/E2
Abdominal	WT	0.25 \pm 0.02 ^b	0.60 \pm 0.10 ^{*,#}	0.33 \pm 0.08 ^b
	p47 ^{phox} KO	0.15 \pm 0.03 ^a	0.56 \pm 0.07 ^{*,#}	0.13 \pm 0.02 ^a
% Body weight	WT	1.00 \pm 0.10	1.80 \pm 0.20 [*]	1.30 \pm 0.20 ^b
	p47 ^{phox} KO	0.80 \pm 0.20	1.70 \pm 0.10 ^{*,#}	0.60 \pm 0.20 ^a
Gonadal	WT	1.10 \pm 0.30 ^b	1.50 \pm 0.10 ^{a,#}	0.80 \pm 0.10 ^b
	p47 ^{phox} KO	0.50 \pm 0.10 ^a	1.90 \pm 0.10 ^{b,*,#}	0.40 \pm 0.10 ^a
% Body weight	WT	4.50 \pm 1.20 ^b	4.40 \pm 0.10 ^{a,#}	3.00 \pm 0.10 ^b
	p47 ^{phox} KO	2.50 \pm 0.50 ^a	5.60 \pm 0.40 ^{b,*,#}	2.00 \pm 0.10 ^a
Subcutaneous	WT	0.10 \pm 0.03	0.20 \pm 0.03 [*]	0.18 \pm 0.05 ^b
	p47 ^{phox} KO	0.08 \pm 0.02	0.20 \pm 0.02 ^{*,#}	0.10 \pm 0.02 ^a
% Body weight	WT	0.40 \pm 0.15	0.60 \pm 0.10	0.70 \pm 0.30
	p47 ^{phox} KO	0.40 \pm 0.15	0.60 \pm 0.10	0.40 \pm 0.10

Note: Data are mean \pm SEM for $n = 6-8$ /group; means with differing letters differ by genotype ($P < 0.05$) within estrogen status a < b.

*Effect of OVX vs. Intact within genotype $P < 0.05$.

#Effect of E2 treatment in OVX groups within genotype $P < 0.05$.

E2: estradiol; OVX: ovariectomized.

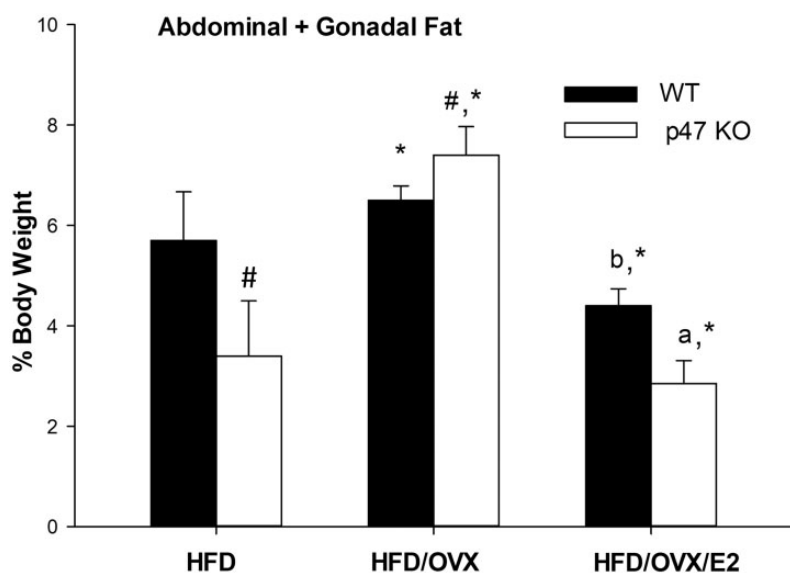


Figure 2. Effects of p47^{phox} genotype and estrogen status on relative weight of visceral fat (abdominal + gonadal fat pads) of female mice fed high fat “Western” diets. WT: wild type; p47 KO: p47^{phox} mouse; HFD: high fat diet; OVX: ovariectomy; OVX E2: ovariectomy with estrogen replacement. [#]*P* < 0.05 HFD/OVX vs. HFD within genotype; ^{*}*P* < 0.05 HFD/OVX vs. HFD/OVX/E2 within genotype; ^b > ^a, *P* < 0.05 genotype within group with same estrogen status. Data are mean ± SEM for *n* = 6–8/group.

Table 2. The relationship between estrogen status, p47^{phox} genotype and mean adipocyte size in gonadal fat pads.

Adipocyte size (μM)	Genotype (%)					
	Wild Type			P47 ^{phox} KO		
	HF	HF/OVX	HF/OVX/E2	HF	HF/OVX	HF/OVX/E2
<3000	15	7	22	22	33	58
3000–4000	13	8	13	16	6	17
4000–5000	16	11	17	20	9	10
>5000	52	71	50	43	47	16

Note: Data are the average % of cells within the μM dimensions listed in *n* = 6–8 mice/group. E2: estradiol; HF: high fat; OVX: ovariectomized.

status and p47^{phox} genotype on visceral fat pad weights, additional effects were observed on the size distribution of adipocytes in the gonadal fat pad (Table 2). HFD p47KO mice had a larger proportion of small adipocytes <3000 μM and a smaller proportion of hypertrophic adipocytes >5000 μM than HFD WT mice. Whereas OVX reduced the proportion of small adipocytes and increased the proportion of large hypertrophic adipocytes in WT mice, this did not occur in OVX p47KO mice. Moreover, after E2 replacement, the effect of p47^{phox} genotype on adipocyte size in HFD-fed mice was particularly evident. HFD/OVX/E2 P47KO mice had 2.6-fold more small adipocytes and 3.2-fold fewer large hypertrophic adipocytes than HFD/OVX/E2 WT female mice.

Interaction between p47^{phox} genotype and estrogen status regulates whole body energy status in female mice fed high fat “Western” diets

No significant effects of genotype *per se* were observed on VO₂ (Table 3). However, the effect of estrogenic status on VO₂ was highly significant (*P* = 0.005) and there was a

significant interaction between genotype and estrogenic status *P* ≤ 0.05 with regards to oxygen consumption. VO₂ was reduced by OVX compared to the intact groups and significantly increased in the OVX + E2 groups. The effect of E2 replacement was greater in the p47KO mice than WT mice. Overall RER and heat production did not differ by genotype or by estrogenic status. However, in both cases, there was a significant interaction between the two. RER and heat production were slightly elevated in Western diet-fed WT mice by OVX and reduced in the OVX + E2 group. In contrast, in p47KO mice, the opposite response to OVX and E2 replacement was observed (interaction *P* = 0.004) (Table 3). No significant effects of genotype, estrogenic status, or interaction between the two were observed on mouse activity as measured in the CLAMS system.

Interaction between p47^{phox} genotype and estrogen status regulates serum leptin and adiponectin levels in female mice fed high fat “Western” diets

Significant interactions between genotype, estrogen status and level of serum adipokines were observed (Table 4).

Table 3. Effect of p47^{phox} genotype and estrogen status on whole body energy utilization.

Outcomes	WT			P47 KO			P-values from ANOVA					
	HF	HF/OVX	HF/OVX/E2	HF	HF/OVX	HF/OVX/E2	Genotype	Diet	HF	HF/OVX	HF/OVX/E2	Interaction
VO2	1 (0.14)	0.96 (0.07)	1.05 (0.08)	1.09 (0.11)	0.81 (0.04)	1.34 (0.08)	0.3324	0.0047*	a, b	b	a	0.0552
RER	1 (0.03)	1.08 (0.01)	1.04 (0.01)	1.08 (0.03)	1.02 (0.02)	1.07 (0.02)	0.2936	0.6503				0.0034*
Heat	1 (0.14)	1.12 (0.07)	0.99 (0.07)	0.99 (0.09)	0.91 (0.04)	1.22 (0.06)	0.9502	0.4135				0.0380*
Activity	1 (0.30)	0.59 (0.07)	1.07 (0.23)	0.97 (0.29)	0.59 (0.14)	0.99 (0.29)	0.8369	0.0874				0.9836

Note: Data are mean (SE) $n = 6-8$ /group; *indicates $P < 0.05$, $b > a$.
OVX: ovariectomized; HF: high fat.

Table 4. Relationship between estrogen status, p47^{phox} genotype, and serum adipokine levels after feeding HFD.

Adipokine	Genotype	Intact	OVX	OVX+E2
Leptin (ng/mL)	Wild Type	24 ± 4 ^b	32 ± 4 ^{a, #}	16 ± 4
	P47 ^{phox} -/-	11 ± 4 ^a	33 ± 4 ^{a, #}	10 ± 5
Adiponectin (μg/mL)	Wild Type	222 ± 43 ^b	350 ± 38 ^{b, *}	106 ± 42
	P47 ^{phox} -/-	153 ± 38 ^a	206 ± 40 ^a	137 ± 42

Note: Data are mean ± SEM for $n = 6-8$ /group; means with differing letters differ by genotype ($P < 0.05$) $a < b$.

*Effect of OVX within genotype ($P < 0.05$).

#Effect of E2 within genotype ($P < 0.05$).

.OVX: ovariectomized; E2: estradiol.

Serum leptin concentrations were lower in intact HFD p47KO mice than in intact HFD WT mice ($P < 0.05$). OVX increased leptin concentrations significantly in both genotypes and there was no genotype difference between OVX groups. E2 treatment reduced serum leptin in both genotypes ($P < 0.05$) but there was no genotype difference between WT OVX+E2 and p47KO OVX+E2 groups. Serum adiponectin values were higher in the intact WT HFD group compared to the intact HFD p47KO group ($P < 0.05$). Moreover, significantly increased adiponectin concentrations after OVX were only observed in the WT group and OVX groups differed by genotype ($P < 0.05$). E2 treatment resulted in reduced adiponectin levels only in the WT group ($P < 0.05$) but adiponectin values did not differ by genotype in OVX+E2 groups.

Interaction of p47^{phox} genotype and E2 signaling affects expression of NOX enzymes in adipose tissue

mRNA expression of the major NOX enzymes expressed in adipose tissue—NOX2 and NOX4—was examined in the gonadal fat pads from mice in the current study by real-time RT-PCR. In both HFD WT and HFD p47KO mice, expression of NOX2 mRNA was elevated 3–4-fold by OVX and suppressed back to the level observed in intact mice by E2 replacement. Overall ANOVA for genotype effect $P = 0.9$; effect of estrogenic status $P = 0.03$; interaction $P = 0.8$. However, the effect of OVX and E2 replacement only reached statistical significance at $P < 0.05$ in the p47KO mice (Figure 3(a)). It should be noted that the increase in NOX2 mRNA could only result in increased NOX2 activity in OVX WT mice since in the absence of p47^{phox} protein in the p47KO mice NOX2 would be unable to form a functional complex. NOX4 mRNA expression did not respond to OVX in HFD WT mice, but was

markedly upregulated by OVX in HFD p47KO mice ($P < 0.05$) (Figure 2(b)). E2 replacement significantly suppressed NOX4 mRNA expression in HFD/OVX p47KO mice ($P < 0.05$). Moreover, NOX4 mRNA expression was lower in HFD/OVX/E2 p47KO mice compared to the HFD/OVX/E2 WT group ($P < 0.05$).

Interaction of p47^{phox} genotype and E2 signaling affects PPAR γ signaling pathways in adipose tissue

There were no significant differences in PPAR γ mRNA expression or expression of mRNA encoding PPAR γ target genes CD36, lipoprotein lipase (LPL), or leptin in the gonadal fat pads of WT mice after OVX or E2 replacement (Figure 4). However, expression of PPAR γ targets was highly responsive to E2 status in p47KO mice. In particular, CD36 and LPL mRNA levels were increased by OVX in HFD p47KO mice relative to intact HFD p47KO mice ($P < 0.05$) and mRNA expression was suppressed in the HFD/OVX/E2 p47KO group relative to the HFD/OVX p47KO group ($P < 0.05$) (Figure 4(b) and (c)). Overall ANOVA for genotype/estrogen status interaction $P = 0.1$ for CD36 and $P = 0.05$ for LPL. LPL mRNA was expressed at higher levels in intact HFD WT mice compared to intact HFD p47KO mice ($P < 0.05$). This genotype effect on LPL mRNA expression was reversed after OVX but then restored in HFD/OVX/E2 WT mice relative to HFD/OVX/E2 p47KO mice ($P < 0.05$) (Figure 4(c)). Expression of leptin mRNA revealed a similar pattern but data were too variable for the genotype/estrogen interaction to reach significance. ANOVA for genotype $P = 0.9$; ANOVA for estrogenic status $P = 0.02$, ANOVA for interaction $P = 0.2$ (Figure 4(d)).

Interaction of p47^{phox} genotype and E2 signaling regulates gonadal adipose tissue pathology developed in response to HFD

It has been shown that when intake of calories/fatty acids exceeds the capacity of fat cells to store the excess energy, some adipocytes undergo cell death in the form of pyroptosis.²⁸ This is characterized by formation of cytosolic inflammasome complexes in response to signaling through danger- or pathogen-associated molecular patterns such as the NOD-like receptor Nlrp3 and the thioredoxin interacting/inhibiting protein txnip.²⁸ Inflammasome complex formation results in proteolysis via caspase 1 and increased expression and processing of inflammatory cytokines, in particular IL-1 β .⁹ Nlrp3 mRNA was expressed more

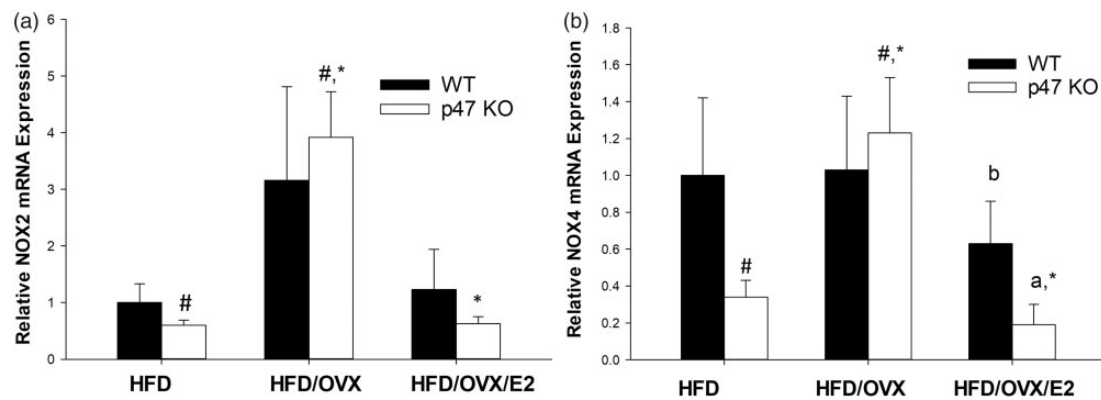


Figure 3. Effects of p47^{phox} genotype and estrogen status on expression of (a) NOX2 mRNA and (b) NOX4 mRNA in gonadal fat pads of female mice fed high fat “Western” diets. WT: wild type; p47 KO: p47^{phox} mouse; HFD: high fat diet; OVX: ovariectomy; OVX E2: ovariectomy with estrogen replacement. #*P* < 0.05 HFD/OVX vs. HFD within genotype; **P* < 0.05 HFD/OVX vs. HFD/OVX/E2 within genotype; b > a, *P* < 0.05 genotype within group with same estrogen status. Data are mean ± SEM for *n* = 6–8/group.

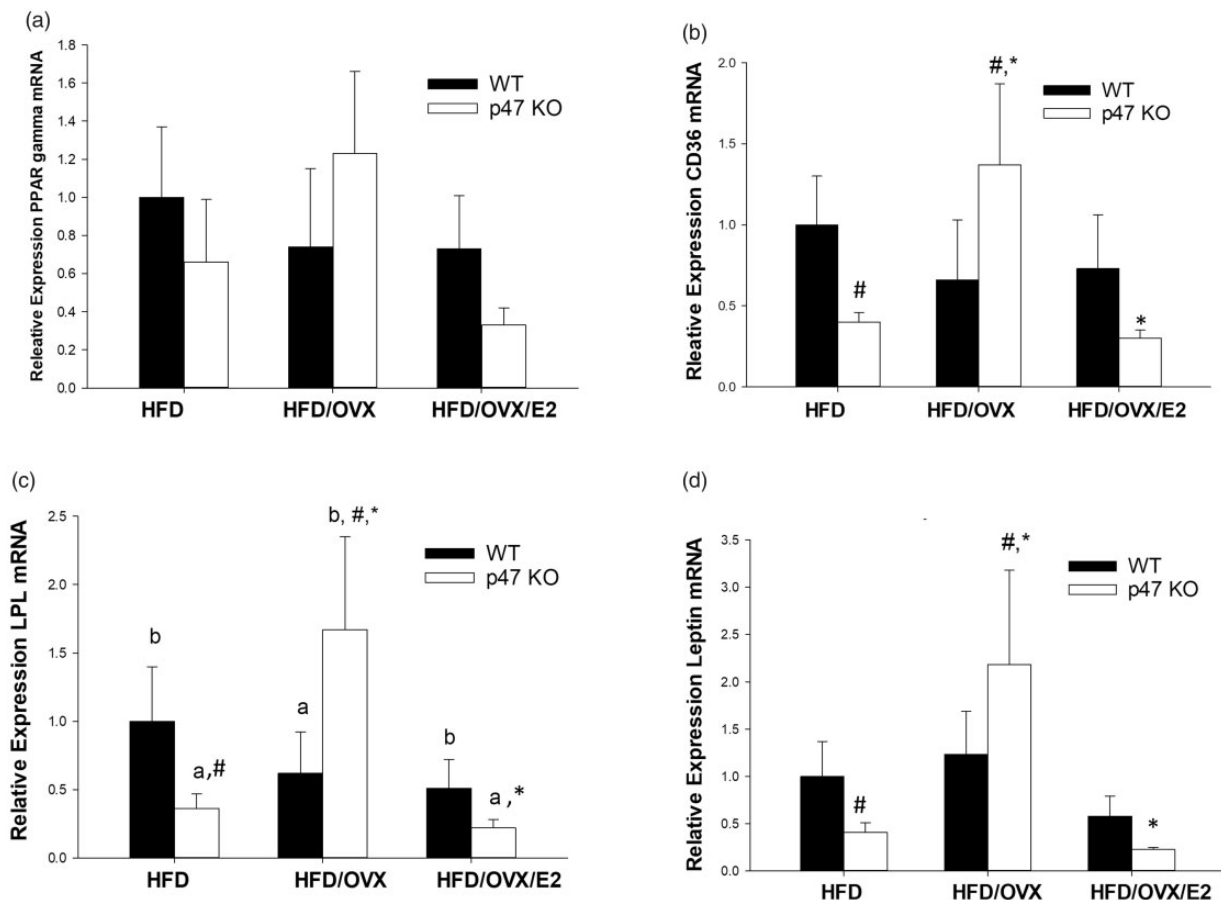


Figure 4. Effects of p47^{phox} genotype and estrogen status on expression of (a) PPARγ mRNA and downstream gene targets – (b) CD36 mRNA; (c) Lipoprotein lipase (LPL) mRNA and (d) leptin mRNA in gonadal fat pads of female mice fed high fat “Western” diets. WT: wild type; p47 KO: p47^{phox} mouse; HFD: high fat diet; OVX: ovariectomy; OVX E2: ovariectomy with estrogen replacement. #*P* < 0.05 HFD/OVX vs. HFD within genotype; **P* < 0.05 HFD/OVX vs. HFD/OVX/E2 within genotype; b > a, *P* < 0.05 genotype within group with same estrogen status. Data are mean ± SEM for *n* = 6–8/group.

highly in gonadal fat from both intact and OVX HFD WT compared to intact and OVX HFD p47KO mice (*P* < 0.05) (Figure 5(a)). Txnip mRNA expression was elevated by OVX. Estrogenic status overall ANOVA *P* = 0.03 but this only achieved statistical significance within genotype in

p47KO mice (Figure 5(b)). Likewise, Tixnip mRNA expression was suppressed significantly by E2 treatment of HFD/OVX mice in p47KO but not WT mice (*P* < 0.05) (Figure 5(b)). Caspase 1 mRNA expression in gonadal fat pads was unaffected by OVX or E2 replacement in HFD WT

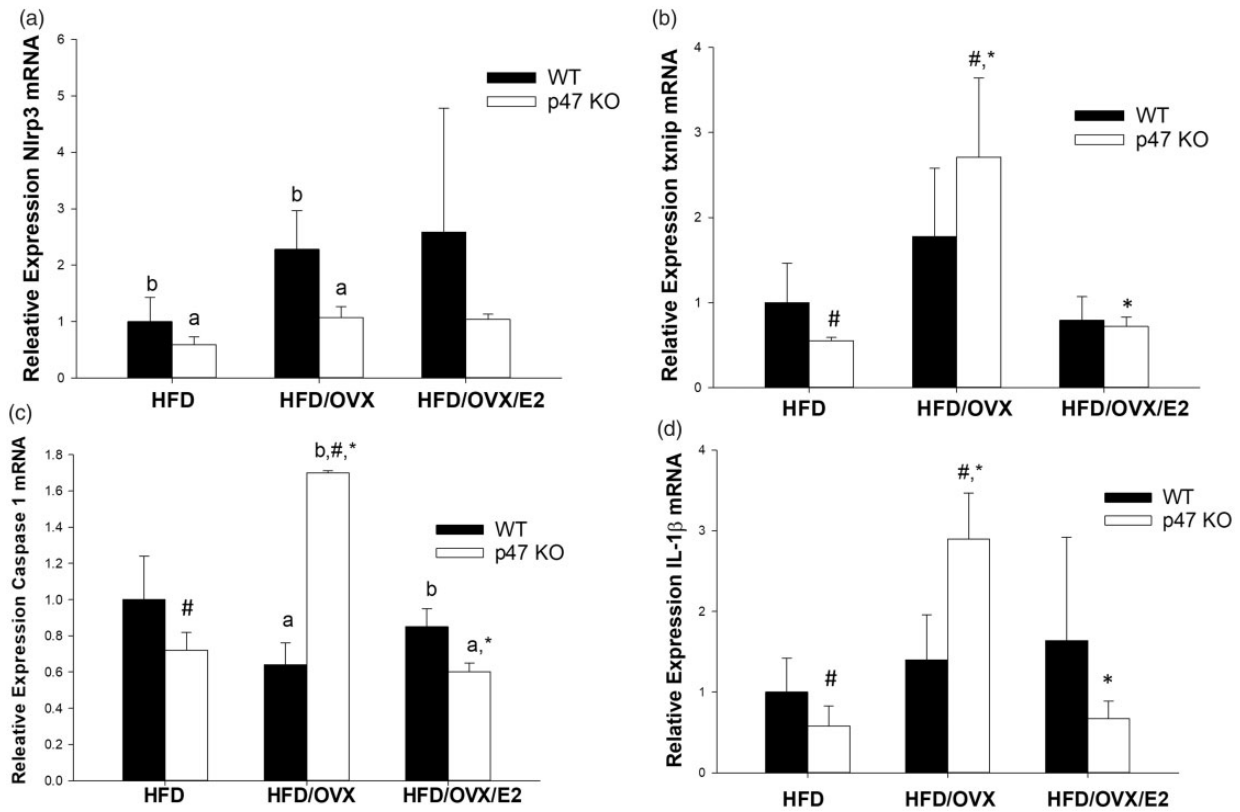


Figure 5. Effects of p47^{phox} genotype and estrogen status on expression of genes involved in adipocyte pyroptosis in the gonadal fat pads of female mice fed high fat "Western" diets. (a) Nlrp3 mRNA; (b) txnip mRNA; (c) Caspase 1 mRNA; (d) Interleukin (IL)1 β mRNA. WT: wild type; p47 KO: p47^{phox-/-} mouse; HFD: high fat diet; OVX: ovariectomy; OVX E2: ovariectomy with estrogen replacement. # $P < 0.05$ HFD/OVX vs. HFD within genotype; * $P < 0.05$ HFD/OVX vs. HFD/OVX/E2 within genotype; b > a, $P < 0.05$ genotype within group with same estrogen status. Data are mean \pm SEM for $n = 6-8$ /group.

mice. However, OVX increased and E2 replacement decreased caspase 1 mRNA expression ($P < 0.05$) in p47KO mice. Caspase 1 mRNA was regulated by estrogen status only in p47KO mice. A significant genotype effect was observed in HFD/OVX mice with greater expression in p47KO mice compared to WT. The genotype effect was reversed in the HFD/OVX/E2 groups where caspase mRNA expression was greater in WT mice (Figure 5(c)). Overall ANOVA for genotype $P = 0.1$, ANOVA for estrogenic status $P = 0.01$, ANOVA for genotype/estrogenic status interaction $P = 0.0002$. IL-1 β mRNA expression was increased by OVX only in the p47KO mice ($P < 0.05$). Moreover, E2 replacement significantly suppressed IL-1 β mRNA expression in p47KO HFD/OVX mice ($P < 0.05$) (Figure 5(d)).

Adipocyte death as a result of HFD was accompanied by pathological and molecular markers of inflammation and ER stress in gonadal fat pads of female mice. These markers were also affected by both E2 status and p47^{phox} genotype and genotype/estrogenic status interactions (Figure 6). In HFD p47KO mice, but not HFD WT mice, mRNA encoding the ER stress marker CHOP10/GADD153 mRNA expression was elevated by OVX and suppressed to levels seen in intact mice by E2 replacement ($P < 0.05$) (Figure 6(a)). Although mean mRNA expression for TNF α in gonadal fat was higher in all treatment groups from WT mice compared to p47KO mice, there was no evidence of E2-specific

regulation (Figure 6(b)). No difference in expression was observed between groups in WT mice. Similar patterns of mRNA expression to GADD153 were observed for IL-6 and RANTES mRNAs in p47KO mice (Figure 6(c) and (d)). However, differences between groups did not reach statistical significance. Expression of mRNA encoding the chemokine Mcp-1 in gonadal fat pads from HFD mice was also affected by interaction between estrogenic status and genotype. Overall ANOVA for genotype $P = 0.9$; ANOVA for estrogenic status $P = 0.08$; ANOVA for interaction $P = 0.04$. Mcp-1 mRNA was greater in intact HFD/WT than intact HFD/p47KO mice ($P < 0.05$) and was greater in WT HFD/OVX/E2 mice relative to p47KO HFD/OVX/E2 mice ($P < 0.05$) (Figure 6(e)). Crown-like structures of macrophages surrounding dead adipocytes were evident in the intact HFD WT group, but absent from the intact HFD p47KO group (Figure 6(f), $P < 0.005$, Figure 7). OVX increased incidence of crown-like structures in both genotypes coincident with increased body weight gain and increased adiposity. However, incidence was lower in HFD/OVX p47KO mice compared to HFD/OVX WT mice ($P < 0.005$). E2 replacement abolished development of crown-like structures in HFD/OVX mice of both genotypes ($P < 0.005$) (Figures 6(f) and 7).

In addition to inflammation, HFD-associated obesity results in matrix remodeling in fat pads and adipose tissue fibrosis characterized by increased expression of

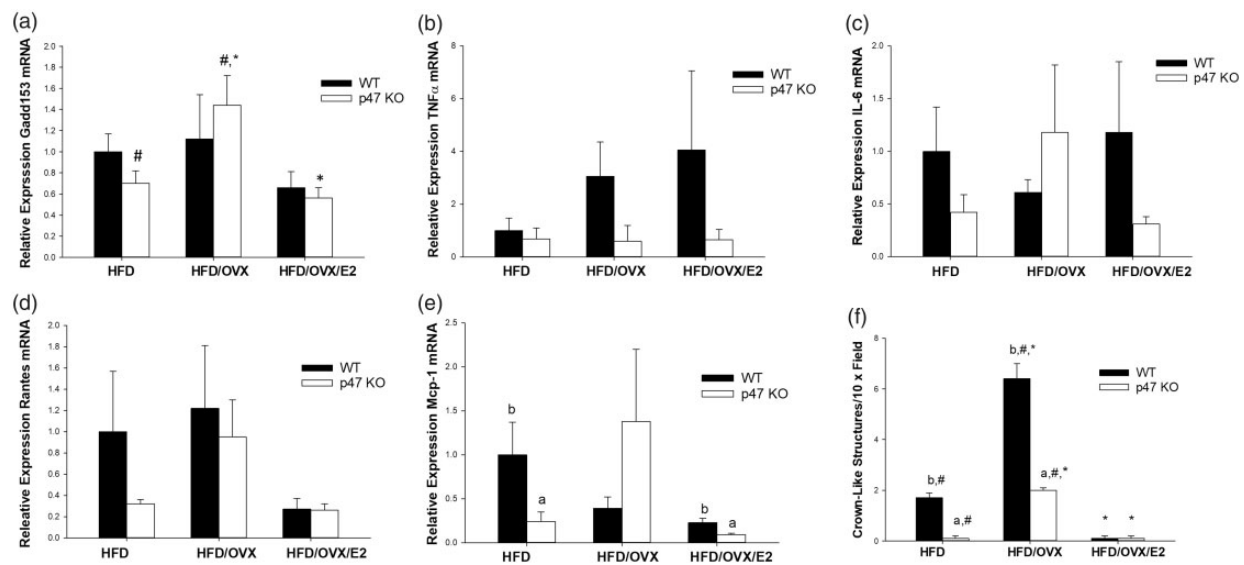


Figure 6. Effects of p47^{phox} genotype and estrogen status on gonadal fat pad inflammation in female mice fed high fat “Western” diets. (a) CHOP/Gad153 mRNA; (b) Tumor necrosis factor (TNF) α mRNA; (c) Interleukin (IL)6 mRNA; (d) Rantes mRNA; (e) Mcp-1 mRNA; (f) Crown-like structures. WT: wild type; p47 KO: p47^{phox} $^{-/-}$ mouse; HFD: high fat diet; OVX: ovariectomy; OVX E2: ovariectomy with estrogen replacement. # $P < 0.05$ HFD/OVX vs. HFD within genotype; * $P < 0.05$ HFD/OVX vs. HFD/OVX/E2 within genotype; b > a, $P < 0.05$ genotype within group with same estrogen status. Data are mean \pm SEM for $n = 6$ –8/group.

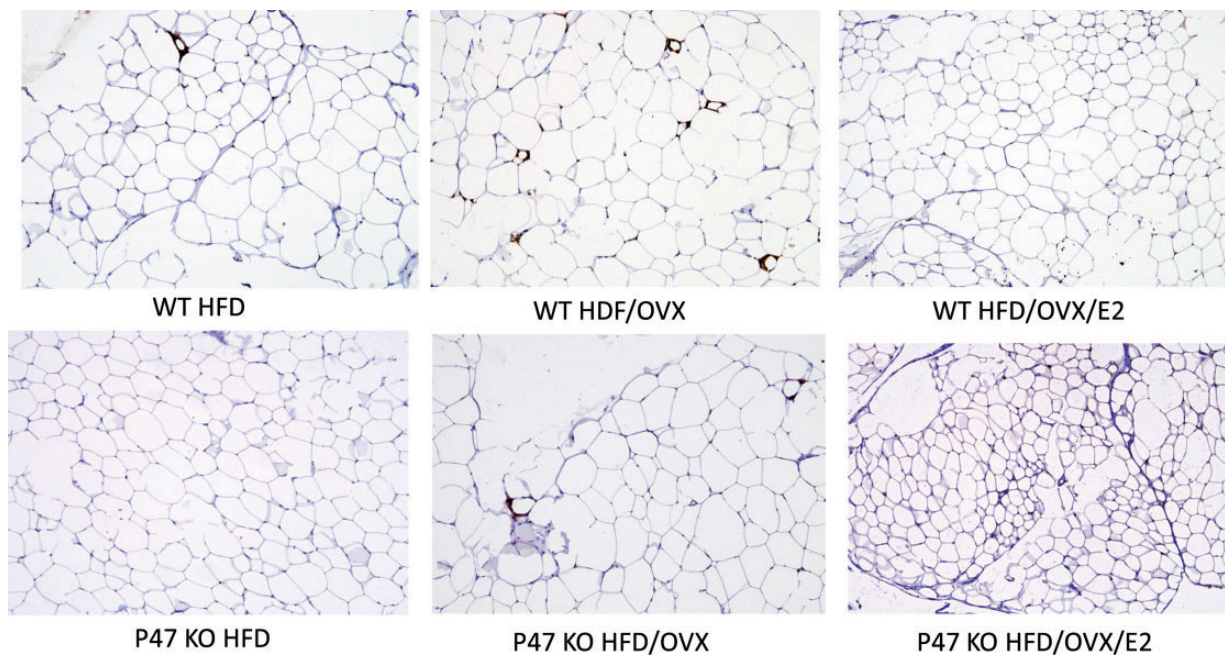


Figure 7. Representative pictures of crown-like structures in gonadal fat pads of female mice fed high fat “Western” diets. WT: wild type; p47 KO: p47^{phox} $^{-/-}$ mouse; HFD: high fat diet; OVX: ovariectomy; OVX E2: ovariectomy with estrogen replacement. (A color version of this figure is available in the online journal.)

matrix metalloproteinases (Mmps) and collagen deposition (5). Expression of Mmp2 mRNA was greater in intact HFD WT than intact HFD p47KO mice and whereas Mmp2 expression was E2 independent in WT mice, E2 regulation was evident in p47KO mice with increases after OVX and suppression by E2 replacement ($P < 0.05$) (Figure 8(a)). Similar expression patterns were observed for collagen 1A1 and collagen 6a3 mRNA (Figure 8(b) and (c)). Expression of both mRNAs was higher in intact HFD WT than intact HFD p47KO mice ($P < 0.05$) and E2 regulation

was only statistically significant after p47^{phox} deletion ($P < 0.05$).

Interaction of p47^{phox} genotype and E2 signaling regulates glucose homeostasis after feeding of HFD

In HFD WT mice, OVX and E2 replacement had little effect on fasting HOMA values or areas under the glucose and insulin time courses following glucose tolerance testing. In contrast, fasting HOMA and plasma glucose values

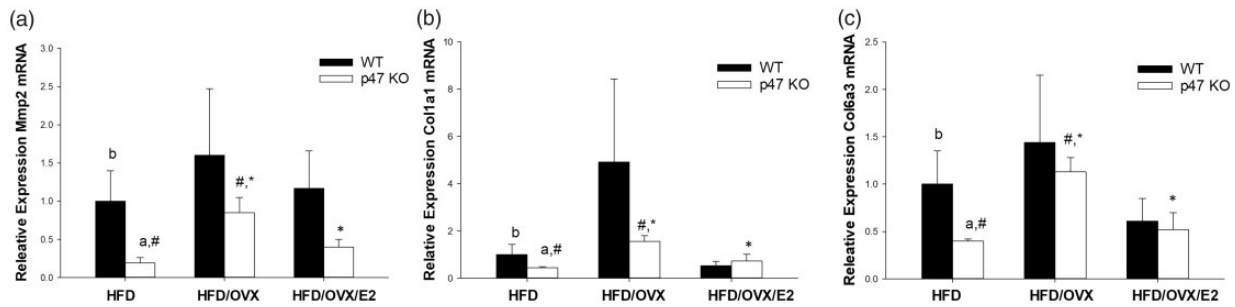


Figure 8. Effects of p47^{phox} genotype and estrogen status on gonadal fat pad markers of matrix remodeling and fibrosis in female mice fed high fat “Western” diets. (a) Mmp2 mRNA; (b) Collagen Col1a1 mRNA; (c) Collagen Col6a3 mRNA. WT: wild type; p47 KO: p47^{phox} mouse; HFD: high fat diet; OVX: ovariectomy; OVX E2: ovariectomy with estrogen replacement. [#] $P < 0.05$ HFD/OVX vs. HFD within genotype; ^{*} $P < 0.05$ HFD/OVX vs. HFD/OVX/E2 within genotype; $b > a$, $P < 0.05$ genotype within group with same estrogen status. Data are mean \pm SEM for $n = 6$ –8/group.

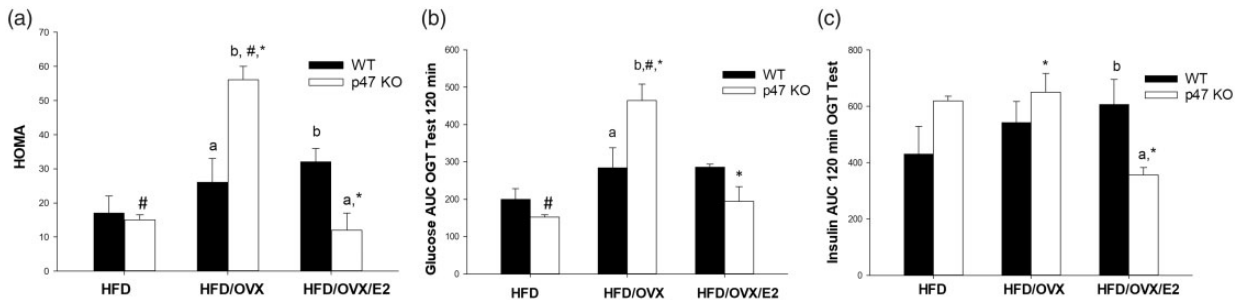


Figure 9. Effects of p47^{phox} genotype and estrogen status on insulin resistance and glucose homeostasis in female mice fed high fat “Western” diets. (a) HOMA values after overnight fast; (b) Area under the 120 min glucose-time curve following glucose injection in oral glucose tolerance test; (c) Area under the 120 min insulin-time curve following glucose injection in oral glucose tolerance test. WT: wild type; p47 KO: p47^{phox} mouse; HFD: high fat diet; OVX: ovariectomy; OVX E2: ovariectomy with estrogen replacement. [#] $P < 0.05$ HFD/OVX vs. HFD within genotype; ^{*} $P < 0.05$ HFD/OVX vs. HFD/OVX/E2 within genotype; $b > a$, $P < 0.05$ genotype within group with same estrogen status. Data are mean \pm SEM for $n = 6$ –8/group.

following the glucose tolerance test were highly regulated by E2 in HFD p47KO mice (Figure 9). Fasting HOMA values and plasma glucose values following the glucose tolerance test were lower in HFD/OVX WT mice than in HFD/OVX p47KO mice ($P < 0.05$) and fasting HOMA was higher in HFD/OVX/E2 WT mice than in HFD/OVX/E2 p47KO mice (Figure 9(a) and (b)) ($P < 0.05$). Overall ANOVA for genotype/estrogenic status interaction $P = 0.006$ for HOMA and $P = 0.01$ for the area under the plasma glucose time course. Moreover, the area under the plasma insulin time course following glucose challenge was higher in HFD/OVX/E2 WT mice than in HFD/OVX/E2 p47KO mice indicating greater insulin resistance in the HFD WT mice under these conditions. Overall ANOVA for genotype/estrogenic status interaction $P = 0.01$.

Discussion

Obesity and chronic feeding of HFD result in appearance of metabolic syndrome including insulin resistance and hyperglycemia.^{7,10} These parameters appear to be highly influenced by NOX genotype/gender interactions. Previous studies from our laboratory have shown that stromal vascular cells from the fat pads of p47KO mice exhibit lower basal and stimulated production of hydrogen peroxide compared to cells from WT mice.²⁶ We and others have demonstrated that global knockdown or inactivation of

NOX2 activity also result in reduced weight gain and adiposity, adipose tissue inflammation and increased insulin sensitivity after high fat feeding.^{22–24,26} These effects appear to be independent of any effects on food intake. Part of the effect appears mediated by NOX2 activity in myeloid cells since targeted myeloid-specific deletion results in lower body weight, reduced adipose tissue inflammation, and delayed adiposity after high fat feeding.²⁵ Additional effects appear due to the role of NOX2-mediated ROS signaling on adipocyte differentiation and whole-body energy expenditure associated with increased expression of mitochondrial respiratory complexes and mitochondrial uncoupling.²⁶ We have shown that the effects of NOX2 inactivation on body composition, energy expenditure, and insulin sensitivity were much greater in female than male mice where the NOX2 cytosolic coactivator p47^{phox} is ablated.²⁶ However, the relative contribution of NOX2 signaling in adipocytes vs. liver or skeletal muscle to these physiological endpoints awaits high fat feeding studies in tissue-specific knockout mice. The current study was designed to determine if the mechanisms underlying the sexual dimorphism in effects of NOX2 inactivation involved negative cross-talk between NOX2 and estrogen signaling pathways. Data in the intact females are consistent with our previous findings demonstrating reduced body weight and gonadal fat pad weight, decreased adipokine production, reduced adipose tissue inflammation and fibrosis markers in p47 KO mice compared to wild type

females fed a high fat "Western diet." Overall, the endpoint differences observed in intact female WT and p47 KO mice either disappeared or were reversed in mice following OVX and the ovariectomy effect was blocked in OVX mice treated with E2, consistent with a role for E2 in maintaining genotype differences between intact WT and p47KO mice. Across multiple parameters, it was evident that the effects of OVX and E2 replacement were also significantly greater in the p47KO mice than in WT mice, suggesting that E2 effects on body composition and insulin sensitivity are significantly attenuated when NOX2-dependent ROS signaling pathways are active. Body weight was increased ($P < 0.05$) in both WT and p47KO mice after OVX, but the genotype difference was abolished. E2 treatment suppressed body weight in both OVX genotypes but significantly reduced body weight gain in the HFD/OVX/E2 p47KO mice relative to HFD/OVX/E2 WT mice became evident with age. Gonadal fat pad weight became greater in OVX p47KO mice than in OVX WT mice while serum leptin values were increased and equalized, effects which were reversed with E2 treatment. Interestingly, serum adiponectin levels remained lower in HFD/OVX p47 KO mice compared to HFD/OVX WT mice suggesting additional levels of regulation. Adipose tissue inflammation, as measured by the appearance of crown-like structures, was increased by OVX in both genotypes but the genotype difference of higher inflammation in WT mice was maintained. Interestingly, E2 treatment abolished adipose tissue inflammation in both genotypes. Consistent with our previous data, in female mice, adipocyte size skewed towards large $>5000 \mu\text{M}$ cells in WT mice of all treatments. In contrast, a larger proportion of adipocytes in p47 KO mice were small $<3000 \mu\text{M}$.²⁶ This was particularly evident in the OVX/E2 p47KO group and was associated with reduced expression of PPAR γ mRNA and downstream gene targets including CD36, lipoprotein lipase, and leptin compared to WT OVX/E2 mice. Expression of NOX2 mRNA itself appears to be estrogen-regulated since it was significantly upregulated by OVX and suppressed by further E2 treatment. In WT, but not p47KO, mice this would be accompanied by increased NOX2-dependent ROS signaling. This might contribute to the large increase in adipose tissue inflammation seen in OVX WT mice. Although little effect of OVX or E2 replacement was seen on NOX4 expression in WT mice, NOX4 was highly regulated by estrogenic status in p47 KO mice. This suggests that NOX signaling can affect expression of other NOX enzymes and is consistent with previously reported results of NOX2 upregulation after NOX4 ablation and vice versa.^{29,30} The substantial upregulation of constitutively active NOX4 expression in OVX p47KO mice could explain the significant increases in markers of adipocyte pyroptosis, adipose tissue inflammation and reduced insulin sensitivity seen in these relative to OVX WT mice. NOX4 expression in adipocytes has previously been linked to increased expression of chemotactic factors, such as MCP-1, and to development of insulin resistance.¹⁸

In conclusion, our data are consistent with our previous studies demonstrating sexual dimorphism in protection against high fat-induced obesity and metabolic syndrome

in NOX2 inactivated p47KO mice. The data suggest that the basis of this sexual dimorphism is negative cross talk between NOX2-dependent ROS signaling and E2 signaling pathways. In addition, the more robust phenotype observed in high fat-fed p47KO mice than in high fat-fed myeloid-specific NOX2 knockout mice points to additional roles of NOX2-signaling in pre-adipocytes in regulation of white adipocyte differentiation and in energy expenditure in other organs such as liver and skeletal muscle. This requires further investigation in high fat-fed mice where ablation of NOX2 is specific to pre-adipocytes, hepatocytes, and myocytes. One difficulty in interpretation of the current data is the apparent compensation of NOX4 for loss of NOX2 activity after OVX. Additional studies where both NOX2 and NOX4 are knocked down are required to completely understand the role of NOX-dependent ROS signaling in regulation of body composition and energy expenditure in the face of high fat feeding. An additional limitation of the current study is that we cannot distinguish ROS-signaling interactions with the different ER signaling pathways. Further studies using ER α , membrane bound ER α , ER β and GPR30-specific agonists or cell-specific knockouts will be required to completely understand the basis of negative cross-talk between these pathways. Our data do suggest that negative cross-talk between NOX-signaling and E2 signaling is associated with regulation of body composition and energy expenditure and that loss of estrogens at menopause contributes to development of visceral obesity, adipose tissue inflammation and fibrosis, and development of metabolic syndrome as the result of increased NOX signaling.

Authors' contributions: MJR and TMB conceived of and designed the study. MNB, KS and MF conducted the animal study and analyses. MJR, KS and MAC analyzed the data and conducted the statistical analysis. MJR drafted the manuscript. MJR, MNB, KS, MF MAC and TMB edited and revised the manuscript and approved the final version.

DECLARATION OF CONFLICTING INTERESTS

The author(s) declare no potential conflicts of interest with respect to the research, authorship or publication of this article.

FUNDING

This article was funded in part by United States Department of Agriculture, Agricultural Service Project 6026–51000-010-05S and by R37 AA018282.

ORCID iD

Martin J Ronis  <https://orcid.org/0000-0002-0116-3771>

REFERENCES

1. Jones ME, McInnes KJ, Boon WC, Simpson ER. Estrogen and adiposity – utilizing models of aromatase deficiency to explore the relationship. *J Steroid Biochem Mol Biol* 2007;**106**:37
2. Cooke PS, Naaz A. Role of estrogens in adipocyte development and function. *Exp Biol Med* 2004;**229**:1127–35

3. Davis KE, Neinast MD, Sun K, Skiles WM, Bills JD, Zehr JA, Zeve D, Hahner LD, Cox DW, Gent LM, Xu Y, V Wang Z, A Khan S, Clegg DJ. The sexually dimorphic role of adipose and adipocyte estrogen receptors in modulating adipose tissue expansion, inflammation and fibrosis. *Mol Metab* 2013;**2**:227–42
4. Foryst-Ludwig A, Clemenz M, Hohmann S, Hartge M, Sprang C, Frost N, Krikov M, Bhanot S, Barros R, Morani A, Gustafsson JA, Unger T, Kintscher U. Metabolic actions of estrogen receptor beta are mediated by a negative cross-talk with PPAR gamma. *PLoS Genet* 2008;**4**:e1000108
5. Kim JH, Cho HT, Kim YJ. The role of estrogen in adipose tissue metabolism: insights into glucose homeostasis regulation. *Endocr J* 2014;**61**:1055–67
6. Mattsson C, Olsson T. Estrogens and glucocorticoid hormones in adipose tissue metabolism. *Curr Med Chem* 2007;**14**:2918–24
7. Magkos F, Mittendorf B. Gender differences in lipid metabolism and the effect of obesity. *Obstet Gynecol Clin North Am* 2009;**36**:245–65
8. Nedungadi TP, Clegg DJ. Sexual dimorphism in body fat distribution and risk for cardiovascular diseases. *J Cardiovasc Trans Res* 2009;**2**:321–7
9. Shi H, Seeley RJ, Clegg DJ. Sexual differences in the control of energy homeostasis. *Front Neuroendocrinol* 2009;**30**:396–404
10. Furukawa S, Fujita T, Shimabukuro M, Iwaki M, Yamada Y, Nakajima Y, Nakayama Y, Makishima M, Matsuda M, Shimomura I. Increased oxidative stress in obesity and its impact on metabolic syndrome. *J Clin Invest* 2004;**114**:1752–61
11. Lee VH, Nair S, Rousseau E, Allison DB, Page GP, Tataranni PA, Bogardus C, Permana PA. Microarray profiling of isolated abdominal subcutaneous adipocytes from obese vs. non-obese Pima Indians: increased expression of inflammation-related genes. *Diabetologia* 2005;**48**:1776–83
12. Lin L, Pang W, Chen K, Wang F, Gengler J, Sun Y, Tong Q. Adipocyte expression of PU.1 transcription factor causes insulin resistance through upregulation of inflammatory cytokine gene expression and ROS production. *Am J Physiol Endocrinol Metab* 2012;**302**:E1550–9
13. Silver AE, Beske SD, Christu DD, Donato ASJ, Moreau KL, Eskurza I, Gates PE, Seals DR. Overweight Obese Humans demonstrate increased vascular endothelial NADPH oxidase – p47(phox) expression and evidence of endothelial oxidative stress. *Circulation* 2007;**115**:627–37
14. Leto TL, Morand S, Hurt D, Ueyama T. Targeting regulation of reactive oxygen species formation by NOX family NADPH-oxidases. *Antioxidants Redox Signal* 2009;**11**:2607–19
15. Anilkumar N, Weber R, Zhang M, Brewer A, Shah A. Nox4 and Nox2 NADPH oxidases mediate distinct cellular redox signaling responses to agonist stimulation. *Arterioscler Thromb Vasc Biol* 2008;**28**:1347–54
16. Piccoli C, D'Aprile A, Ripoli M, Scrima R, Lecce L, Boffoli D, Tabilio A, Capitanio N. Bone-marrow derived hematopoietic stem/progenitor cells express multiple isoforms of NADPH oxidase and produce constitutively reactive oxygen species. *Biochem Biophys Res Commun* 2006;**353**:965–72
17. Serrander L, Cartier L, Bedard K, Banf B, Lardy B, Plastre O, Sienkiewicz A, Forro L, Schlegel W, Krause K-H. NOX4 activity is determined by mRNA levels and reveals a unique pattern of ROS generation. *Biochem J* 2007;**406**:105–14
18. Han CY, Umemoto T, Omer M, Den Hartigh LJ, Chiba T, LeBoeuf R, Buller CL, Sweet IR, Pennathur S, Abel ED, Chait A. NADPH oxidase-derived reactive oxygen species increases expression of monocyte chemotactic factor genes in cultured adipocytes. *J Biol Chem* 2012;**287**:10379–93
19. Den Hartigh LJ, Omer M, Goodspeed L, Wang S, Wietecha T, O'Brien KD, Han CY. Adipocyte-specific deficiency of NADPH oxidase 4 delays the onset of insulin resistance and attenuates adipose tissue inflammation in obesity. *Arterioscler Thromb Vasc Biol* 2017;**37**:466–75
20. Li Y, Mouche S, Sajic T, Veyrat-Durebex C, Supale R, Pierroz D, Ferrari S, Negro F, Hasler U, Feraill E, Moll S, Meda P, Deffert C, Montet X, Krause KH, Szanto I. Deficiency in the NADPH oxidase 4 predisposes towards diet-induced obesity. *Int J Obes* 2012;**36**:1503–13
21. Bettqieb A, Jiang JX, Sasaki Y, Chao T-I, Kiss Z, Chen X, Tian J, Katsuyama M, Yabe-Nishimura C, Xi Y, Szyndralewicz C, Schroder K, Shah A, Brandes RP, Haj FG, Torok NJ. Hepatocyte nicotinamide adenine dinucleotide phosphate reduced oxidase 4 regulates stress signaling, fibrosis and insulin sensitivity during development of steatohepatitis in mice. *Gastroenterology* 2015;**149**:468–80
22. Costford SR, Castro-Alves J, Chan KL, Bailey LJ, Woo M, Belsham DD, Brumel JH, Klip A. Mice lacking NOX2 are hyperphagic and store fat preferentially in the liver. *Am J Physiol Endocrinol Metab* 2014;**306**:E1341–53
23. Pepping JK, Freeman LR, Gupta S, Keller JN, Bruce-Keller AJ. NOX2 deficiency attenuates markers of adipopathy and brain injury induced by high fat-diet. *Am J Physiol Endocrinol Metab* 2012;**304**:E392–404
24. Xu X, Yavar Z, Verdin M, Ying Z, Mihai G, Kampath T, Wang A, Zhong M, Lippmann M, Chen LC, Rajagopalan S, Sun Q. Effect of early particulate air pollution exposure on obesity in mice: role of p47phox. *Arterioscler Thromb Vasc Biol* 2013;**30**:2518–27
25. Pepping JK, Vandanmagsar B, Fernandez-Kim SO, Zhang J, Mynatt RL, Bruce-Keller AJ. Myeloid-specific deletion of NOX2 prevents the metabolic and neurologic consequences of high fat diet. *PLoS One* 2017;**12**:e0181500
26. Ronis MJJ, Sharma N, Vantrese J, Borengasser SJ, Ferguson M, Mercer KE, Cleves MA, Gomez-Acevedo H, Badger TM. Female mice lacking p47phox have altered adipose tissue gene expression and are protected against high fat-induced obesity. *Physiol Genomics* 2013;**45**:351–66
27. Rozman J, Rathkolb B, Neschen S, Fuchs H, Gailus-Durner V, Klingenspor M, Wolf E, Hrabě de Angelis M. Glucose tolerance tests for systematic screening of glucose homeostasis in mice. *Curr Protoc Mouse Biol* 2015;**5**:65–84
28. Giordano A, Murano I, Mondini E, Perugini J, Smorlesi A, Severi I, Barazzoni R, Scherer PE, Cinti S. Obese adipocytes show ultrastructural features of stressed cells and die of pyroptosis. *J Lipid Res* 2013;**54**:2423–36
29. Sasaki H, Yamamoto H, Tominaga K, Masuda K, Kawai T, Teshima-Kondo S, Matsuno K, Yabe-Nishimura C, Rokutan K. Receptor activator of nuclear factor-kappaB ligand-induced mouse osteoclast differentiation is associated with switching between NADPH oxidase homologues. *Free Radic Biol Med* 2009;**47**:189–99
30. Watt J, Alund AW, Pulliam CF, Mercer KE, Suva LJ, Chen JR, Ronis MJJ. NOX4 deletion in male mice exacerbates the effect of ethanol on trabecular bone and osteoblastogenesis. *J Pharmacol Exp Ther* 2018;**366**:4

(Received February 19, 2019, Accepted May 8, 2019)